The static and dynamic response of SU-8 electrothermal microgrippers of varying thickness

L.E. Dodd, S.C. Ward, M.D. Cooke and D. Wood
School of Engineering and Computing Sciences, Durham University, South Road, Durham, DH1
3LE, UK
Email: david.wood@durham.ac.uk

Keywords: microgripper, electrothermal actuation, SU-8, simulation, thermal imaging

Abstract
This work presents an investigation into the effect on dynamic response of SU-8 microgrippers due to varying thickness, and subsequent validation via COMSOL Multiphysics simulations and thermal camera profiling during actuation. The tweezer-like microgrippers can easily manipulate, with a high degree of control, cells and particles with diameters as small as 10 μm, without using an impractical operating voltage or generating excessive heat.
However, in order to fully exploit the versatility of the devices, their response characteristics must be fully understood as material and/or dimension parameters change. Therefore an investigation took place to determine the effects of device thickness on functionality of the device, including the drive current required to actuate the gripper and the speed of actuation. Furthermore, an infrared camera was used to characterize the thermal response of the device. Finally, a simulation of the temperature profile and deflection dimension has been developed in order to verify the findings and further investigate and predict the effects of design variations.

1. Introduction

In recent years there has been an increasing need for the precise manipulation of oocyctes for the purposes of Assisted Reproduction Technology (ART), including Intracytoplasmic Sperm Injection (ICSI) and In Vitro Fertilisation (IVF) due to both advancements in techniques and improvement in availability of procedures. With the success rates of ART procedures at 21.7% [1] and the need for oocyte manipulation for use in other areas of scientific research [2], such as cancer treatment and cloning there is a continued need for advancement of design and optimization of micro manipulation devices.

A large amount of work has been produced on the development of microactuators of a variety of intended applications. The method of actuation has predominantly been either electrothermal expansion or electrostatically driven devices. However electrostatically operated microgrippers, relying on parallel plate capacitor combs, have shown limited success for use in the field of micromanipulation. The design presented in [3] showed promise when a 20 μm deflection was achieved. However the 80 V drive regime necessary to operate the design limited the device's suitability for temperature sensitive applications, such as cell handling. The deflection was not sufficient to handle 55 μm oocytes [4]. Despite only achieving limited deflection a use was found in 2005 for blood vessel manipulation [5]. These grippers achieved a maximum deflection of only 22.2 μm but proved successful as the simplified design achieved more reliable fabrication, although a limitation was the 185 V driving voltage.

A greater maximum deflection of 100 μm could be obtained from a double u-shaped electrothermal design [6]. The design employs asymmetrical heating and thermal expansion of two arms of a pseudo-bimorph actuator structure. This produces in-plane deflection and rotation of the gripper arms, thus opening and closing the gripper by forced heating and passive cooling. With tip temperatures approximated to 100 °C, the gripper design remained unsuitable for oocyte manipulation as the enzymes would be denatured [7]. Lower temperature operation, in the range of 10–32 °C, was achieved in [8] but only at deflections of up to 12 μm. Further work was done on attempting to balance low operating temperatures with large maximum deflection, including [9-12]. None demonstrated significant deflection without excessive operating temperatures.

We first reported our microgripper design in 2007 [13]. The microgripper device described here managed to achieve a significant increase in deflection, to 300 μm with tip temperatures near ambient. This was

done by placing the complete heating element track down the "hot" arm of the microgripper, thus removing the parasitic effects of the "cold" arm. This advancement meant that this microgripper proved suitable for oocyte manipulation [14, 15].

The device can grip objects with zero apparent damage, which is achieved by tailoring the microgripper tips at the mask design stage so that they best fit the item being manipulated, with various different tip designs having already been successfully tested. Furthermore, the grippers can have additional functionality added to their design, such as an electrode for electrochemical analysis.

In other work reported previously, we have modelled and experimentally verified the heat loss mechanism in the microgripper [16], performed further heat loss studies in different ambient gases over a range of pressures [17] and demonstrated the use of the microgripper in holding a cell while simultaneously being able to detect and quantify the excretion of potassium ions using an ion specific electrode fabricated as an integral part of the structure [18].

The microgripper device relies on the use of SU-8, which is a negative photoresist polymer that is often used in MEMS devices that require a high aspect ratio, as shown in [19]. The 2000 series contains a variation of the SU-8 polymer, which allows for a large range of thicknesses to be achieved with well-defined sidewall profiles. The variation in thickness is controlled by the viscosities of the different SU-8 solutions available, with layer thickness increasing with viscosity. Finer control of the thickness is achieved through altering the time and velocity of the spinning process when depositing the SU-8. The mechanical properties of SU-8 are heavily controlled by the extent of the cross linking between polymer molecules achieved during the fabrication process [21].

The microgripper used in this investigation was a 100 μm gap, flat tipped structure, with a 'normally open' configuration (tracks on the outside of gripper arms). The structure consisted of a bottom SU-8 2002 layer, gold tracks and a top SU-8 2025 layer. The thickness of microgripper devices was varied via controlling the spin speed during the deposition of the SU-8 2025 layer and the subsequent effects of device performance are explained and compared with COMSOL Multiphysics simulation results of the same structure.

2. Experimental Details
2.1 Device Fabrication

The fabrication steps are described below, with standard UV photolithography used to define each layer.

2.1.1. Oxidation

<100> Silicon wafers are first prepared in $H_2SO_4:H_2O_2$ solution for 20 minutes to remove the native silicon oxide on the wafer, with a final etch in HF. A 0.1 μm thick silicon oxide layer is grown using thermal oxidation. The oxide is patterned using SPR-350 positive photoresist. The exposed silicon oxide is then etched using HF, which defines a layer where the gripper arms will later be.

2.1.2. SU-8 2002

A layer of SU-8 2002, a low viscosity variant of the 2000 series negative photoresist, is spun onto the substrate, resulting in a 1.7 μm thick layer of SU-8. The wafer then undergoes a soft bake process at 65 °C, 95 °C and then 65 °C for 1 minute each. The SU-8 covered substrate is exposed, through a patterned mask, to UV light for a known energy dose. A post-exposure bake then takes place, followed by the development of the pattern on the substrate using EC solvent. A final hard bake at 115 °C cures the polymer.

2.1.3. Metallisation and electroplating

A 25 nm layer of chromium and 100 nm layer of gold are deposited onto the wafer using e-beam evaporation. This metallisation is then patterned using AZ4562 photoresist, and selected regions of the gold layer are thickened using electroplating. These regions correspond to the device's electrical contacts. The gold is pulse electroplated using Neutronex 309 for 90 minutes, resulting in a 5 μm layer of gold. The gold is then patterned into the shape of the gripper design using photolithography, gold etch (4:1:8 $KI:I:H_2O$) and chromium etch (9:1:49 ceric ammonium nitrate:$HNO_3:H_2O$).

2.1.4. SU-8 2025

The SU-8 2025 layer is then spun on to the substrate, followed by a 10 minute rest period to allow for the back fill of air pockets created when spinning differing step heights, resulting

in increased uniformity of the film thickness. The bake procedure involves a 3 minute temperature ramp from ambient to 65 °C, with 1 minute at this temperature. This is followed by a 3 minute ramp from 65 °C to 95 °C and 3 minutes at 95 °C. The wafer is then allowed to cool for 45-60 minutes, returning to ambient.

The SU-8 is then exposed to UV through a patterned mask and a 360 nm optical filter to ensure a vertical side wall profile after development. The sample then undergoes a post exposure bake, which consists of a 3 minute temperature ramp from room temperature to 65 °C, where it is held for 1 minute and then undergoes a 3 minute temperature ramp to 95 °C, held for 4 minutes, and then placed at 65 °C for 1 minute.

The resulting pattern is developed in EC solvent for 6 minutes, followed by a hard bake at 110 °C to cure the polymer.

The spin speed was varied for the purposes of this work, to produce a variety of gripper thicknesses. All wafers were first spun at 2000 rpm, with an additional spin cycle of 2000, 3000, 4000, or 5000 rpm performed on each of the four wafers.

2.1.6. Tip release

To release the gripper arms from the silicon wafer, the silicon oxide patterned earlier in the fabrication process must be etched. This is done using a xenon difluoride vapour phase etcher. It is first ensured that no water vapour is present by cycling N_2, as the etch reacts strongly with water. The wafer is then etched using XeF_2 vapour cycled every 60 s with N_2 for up to 300 cycles. This process releases the gripper arms so that they are freestanding in air and etches along the side edges for the grippers, allowing the wafer to be separated into individual microgripper devices. Pressure is applied along the direction of the etch and a crack propagates along the line of the etch. At this stage the substrate underneath the gripper arms is removed completely, with the arms attached to the base structure. A representation of the final device can be seen in Figure 1, which is a 3D render created in the open source program Blender, with the base structure of the gripper, complete with the actuation tracks clearly visible above the arms, which are free standing. Releasing the gripper arms using the etching technique results in

structures that are unrestricted and able to move freely when actuated electrically.

The gripper arms are either 'normally open' and actuated to close, or 'normally closed' and actuated to open. This is determined by the position of the electrical track within the arm. If this track is on the outside of the arm, as seen in Figure 1, then the device is normally open and during actuation, when each of the 'hot' arms containing the tracks has a current through it, the resultant increase in temperature will cause expansion, resulting in the gripper arms closing. As can be seen in Figure 3, the hottest point of the gripper arm, reaches 106 °C, while the gripper tip is not heated in any way, ensuring that any biological samples are not damaged during handling.
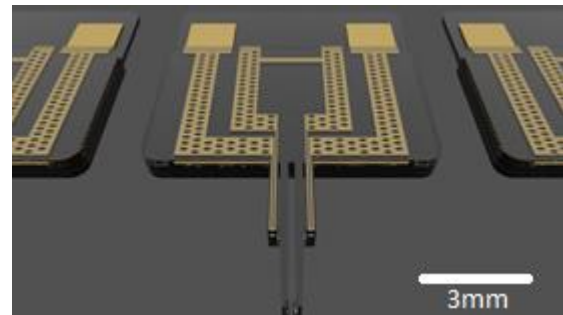
Figure 1 - Representation of microgripper layout

2.2 Device Testing

In order to establish the optimum thickness of the device, a compromise must be sought between structural integrity of the gripper arms, speed of actuation and temperature of the gripper arm tips using both fabricated devices and a COMSOL Multiphysics simulation to verify the results. This was achieved by varying the thickness of the top SU-8 layer, which was the dominant layer in the overall device thickness. A known current was applied across devices of different thicknesses, varying from 20 μm to 80 μm thick (Figure 2), while recording the end deflection using a camera mounted on a standard Nikon optical microscope. The deflection was measured using a counting-pixels methodology, scaling the deflection based on a subsequent measurement of the 'open' gap to calibrate. The measurements are accurate to the nearest pixel within the image (18 μm per pixel for infrared camera, and typically ~1 μm per pixel for optical microscope). The deflection can be seen in

Figure 3, where the gripper tips are close to touching.
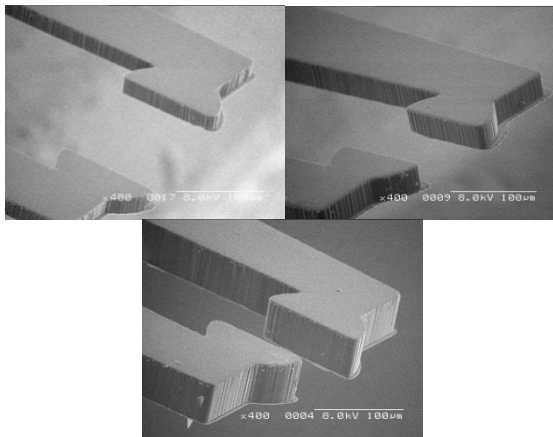
Figure 2 - SEM images showing the difference in device thickness for a top SU-8 layer spun at 5000, 3000 and 2000 rpm (left, right and centre respectively)

Furthermore, in order to ensure that any biological samples, which are to be manipulated by the microgripper device, are not thermally affected by the device actuation, the temperature profile of the device down each of the gripper arms was investigated. A ThermoVision A40 infrared camera with an 18 micron special resolution macro lens was used to investigate the device before and during actuation, to determine the deflection and speed of actuation and the temperature profile of the device as different currents are applied. The measurements are taken under the infrared camera, with the gripper positioned directly below the camera lens, the image is focussed, and then images are taken during the actuation process. For Figure 3, 13 mA current was applied to the device, resulting in the temperature profile and deflection seen.

In order to fully validate the COMSOL model and confirm the temperature of the gripper arms at the tips, thermal camera images have been used. These do confirm that the ends of the gripper arms do not increase in temperature during actuation, and therefore our microgrippers are a viable solution for the manipulation of biological, temperature sensitive samples, as seen in Figure 3. The COMSOL simulations agree with the thermal camera images, they both show that the tips of the gripper arms remain at ambient temperature, as required for biological samples. Given the close nature of the COMSOL model and experimental results, the simulations have since been used to

successfully predict the effects of varying device geometry and could therefore be used as a tool to investigate further device changes prior to manufacture.
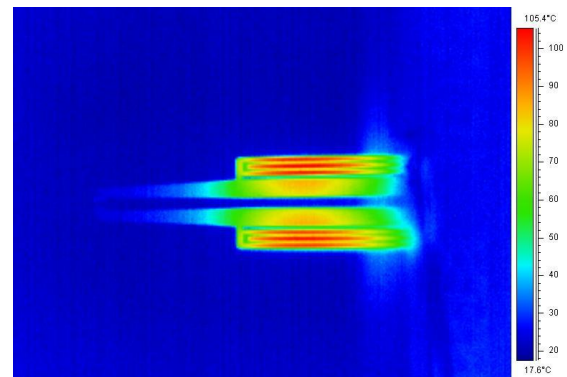
Figure 3 - Thermal camera image of microgripper device, actuated at 13 mA

3. Results and Discussion

As can be seen in Figure 4 and Figure 5, the applied current affects the amount of displacement within the gripper arms, with thinner devices being affected more for the same current than thicker devices. Figure 4 shows the deflection versus time for a 22 μm thick microgripper device, with a simulated thermal conductivity of 3 W/mK, compared to a stated value of 0.3 W/mK [20], the different between which can be attributed to the non-standard baking procedures in this process and the age of the SU-8 used.

Figure 4 shows how the time taken by the gripper arm to move is a function of the applied current, with the settling time being longer for a larger applied current. This is intuitively true, as a larger current will involve a higher temperature, which will take longer to be achieved. As expected, Figure 4 also shows that applying more current results in a greater deflection, due to this larger temperature value. As a result of the close correlation between the experimental and simulated findings, hereafter it can be assumed that the 22 μm device in COMSOL is equivalent to the 4000 rpm spin speed fabricated device.

Figure 5 shows the same amount of current being applied to devices of differing thicknesses. As can be seen, thicker devices deflect less than thinner ones, for a given current. Figure 5 shows a close correlation between experimental and simulated results.

In Figure 4 and in Figure 5, both the experimental results and the COMSOL

simulation results can be seen, with good agreement between both.
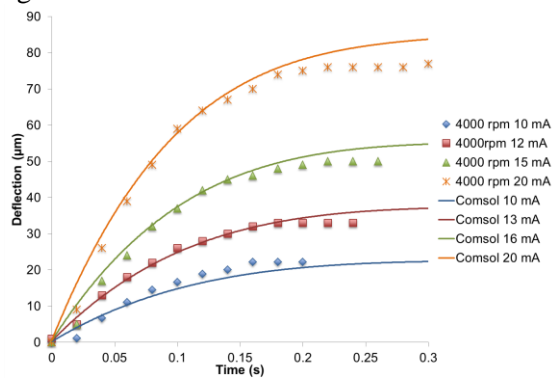
Figure 4 - Graph showing the effect of applied current on a 22 μm thick microgripper
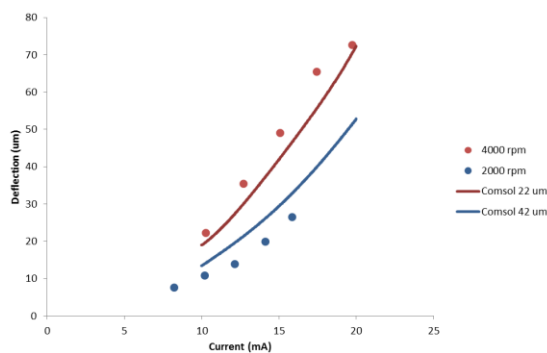
Figure 5 - Graph showing the effect of applied current on gripper arm deflection

COMSOL has also been used to determine the effects of the thickness of the top SU-8 layer on the speed of actuation of the arms. As can be seen in Figure 6, the thicker the SU-8 layer of the gripper device, the slower the actuation of the gripper arms. It is worth noting that the 4000 rpm, 10 mA data from Figure 4 is the same as the 4000 rpm data from Figure 6. A close correlation between COMSOL and experimental results is also apparent. The use of simulation software provides a greater understanding into the response of the microgripper devices and allows for the validation of the COMSOL model used to estimate response of new designs, speeding up future design improvements.
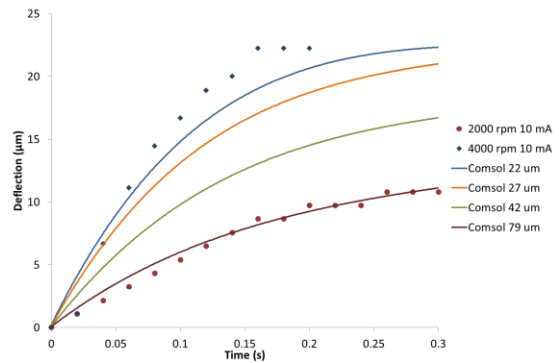
Figure 6 - Graph showing settling time during actuation for different device thicknesses

4. Conclusions

Electrothermally actuated microgripper devices have been fabricated and tested. The thickness of the microgripper devices has been varied and the effects investigated. The thickness of the device affects the speed of actuation and the amount of deflection for a given current. It was also shown that the speed of actuation is also affect by a change in applied current, as seen in Figure 4.

The graphical comparisons between the experimental and simulated results can be seen in Figures 4, 5 and 6, with good agreement between the two sets of results. As a result the simulation can be used to predict future findings, prior to the design of the device and experimental testing.

5. Acknowledgements

6. References

[1] E.S.o.H.R.a. Embryology, eshre.eu, ESHRE, 2013. [Online]. Available: http://www.eshre.eu/Guidelines-and-Legal/ART-fact-sheet.aspx. [Accessed 16 January 2014].
[2] C. Yi, C-W. Li, S. Ji and M. Yang, Microfluidics technology for manipulation and analysis of biological cells, Anal. Chim. Acta, 560 (2006), 1-23.
[3] B. Volland, H. Heerlein and I. Rangelow, Electrostatically driven microgripper, Microelectron. Eng., 61 (2002), 1015-1023.

[4] Y. Hirao and T. Miyano, Oocyte Size at the beginning of Culture Influences the Appropriate Length of Culture Period, J. Mammal. Ova Res., 25 (2008), 56-62.

[5] R. Wierzbicki, K. Houston, H. Heerlein, W. Barth, T. Debski, A. Eisenberg, A. Menciassi, M. Carrozza and P. Dario, Design and fabrication of an electrostatically driven microgripper for blood vessel manipulation, Microelectron. Eng., 83 (2006), 1651-1654.

[6] N.-T. Nguyen, S-S. Ho and C. L.-N. Low, A polymeric microgripper with integrated thermal actuators, J. Micromech. Microeng., 14 (2004), 969-974.

[7] R. M. Daniel, M. Dines and H. H. Petach, The denaturation and degradation of stable enzymes at high temperatures, Biochem. J., 317 (1996), 1-11.

[8] N. Chronis and L. Lee, Electrothermally activated SU-8 microgripper for single cell manipulation in solution, J. Microelectromech. Syst., 14 (2005), 857-863.

[9] T. Duc, G. Lau, J. F. Creemerl and P. Sarrol, Electrothermal Microgripper with large jaw displacement and integrated force sensors, Proc. IEEE MEMS 2008, Tucson, USA, 13-17 (2008), 519-522.

[10] T. Duc, G. Lau and P. M. Sarro, A Nano Initiator Realised by Integrating Al/CuO-Based Nanoenergetic Materials With a Au/Pt/Cr Microheater, J. Microelectromech. Syst., 17 (2008), 823-831.

[11] K. Kim, X. Liu, Y. Zhang and Y. Sun, Nanonewton force-controlled manipulation of biological cells using a monolithic MEMS microgripper with two axis force feedback, J. Micromech. Microeng., 18(2008), article 055013.

[12] K. Colinjivadi, J. Lee and R. Draper, Viable cell handling with high aspect ratio polymer chopstick gripper mounted on a nano precision manipulator, Microsyst. Technol., 14 (2008), 1627-1633.

[13] B. Solano and D. Wood, Design and Testing of a Polymeric Microgripper for Cell Manipulation, Microelectronic Engineering 84 (2007), 1219-1222.

[14] B. Solano, A. J. Gallant and D. Wood, Design and Optimisation of a Microgripper: Demonstration of Biomedical Applications using the Manipulation of Oocytes, Proc 10th Symposium on Design, Test, Integration and Packaging of MEMS and MOEMS, Rome, Italy, (2009), 61-65.

[15] R. Daunton, A. J. Gallant and D. Wood, Manipulation of 10-40 µm Diameter Cells Using a Thermally Actuated Microgripper, Proc Materials Research Society Meeting, San Francisco, USA, 1463 (2012), mrss12-1463-qq02-10.

[16] B. Solano, S. Rolt and D. Wood, Thermal and Mechanical Analysis of an SU8 Polymeric Actuator using IR Thermography, Proc Inst Mech Engrs, 222 (2008), 73-86.

[17] B. Solano, J. Merrell, A. J. Gallant and D. Wood, Modelling and Experimental Verification of Heat Dissipation Mechanisms in an SU-8 Electrothermal Microgripper, Microelectronic Engineering 124 (2014), 90-93.

[18] R. Daunton, D. Wood, A. J. Gallant and R. Kataky, A Microgripper Sensor Device Capable of Detecting Ion Efflux from Whole Cells, RSC Advances 4 (2014), 50536-50541.

[19] J. M. Williams and W. Wang, Study on the postbaking process and effect on UV lithography of high aspect ratio SU-8 microstructures, J. Micro/Nanolithogr. MEMS MOEMS, 3 (2004), 563-568.

[20] Microchem., SU-8 2000 Permanent Epoxy Negative Photoresist. Processing Guildlines for SU-8 2002, Microchem., [Online]. Available: http://www.microchem.com/pdf/SU-82000DataSheet2000_5thru2015Ver4.pdf. [Accessed 22 March 2014].

[21] R. Feng and R. J. Farris, Influence of processing conditions on the thermal and mechanical properties of SU-8 negative photoresist coatings, J. Micromech. Microeng., 13 (2003), 80-88.